Wearable Sensors and Machine Learning for Field-Based Biomechanical Load Assessment in Sports: A Structured Overview of Current Research

Bernd J. Stetter[*1], Julia Unger[1], Stefan Sell[1 2], Thorsten Stein[1]

[1] Institute of Sports and Sports Science, Karlsruhe Institute of Technology, Karlsruhe, Germany
[2] Joint Center Black Forest, Hospital Neuenbuerg, Neuenbuerg, Germany

[*] bernd.stetter@kit.edu

ORIGINAL ARTICLE

Submitted: September 27, 2025

Accepted: April 17, 2026

Published: June 29, 2026

Editor-in-Chief

Claudio R. Nigg, University of Bern, Switzerland

Guest Editors

Thorsten Stein, Karlsruhe Institute of Technology, Germany

Bernd Stetter, Karlsruhe Institute of Technology, Germany

ABSTRACT

The field-based assessment and management of biomechanical load, such as joint forces, in sports has high significance for effective athletic training and prevention of injuries. Developments in wearable sensors and machine learning have improved assessment methods, as they enable measurements in real training or competition environments outside the laboratory. This review systematically summarizes the current state of research on wearable sensors combined with machine learning for assessing biomechanical load in sports. Searches were conducted in PubMed and SPORTDiscus. A total of 5,426 articles were identified, of which 42 met the eligibility criteria after screening. Data were extracted on participant characteristics, sports and movement tasks, wearable sensors used, machine learning methods, model input and biomechanical output, validation strategies, and key findings. Running was the most frequently studied sport, although nine other sports were also investigated. Artificial neural networks and linear regression were the most commonly applied machine learning methods. Biomechanical load was most frequently assessed using ground reaction force metrics, followed by movement execution metrics and joint moment metrics. Current studies highlight that wearable sensors and machine learning can predict biomechanical loads, especially in the lower extremities during running. Expanding the diversity of sports studied and improving sensor placement on the upper extremities are necessary to broaden the application of wearable sensors and machine learning for athlete monitoring and injury prevention in real-world settings.

Keywords

biomechanics, sports, artificial intelligence, wearables, performance, training, injury risk

Citation:

Stetter, B. J., Unger, J., Sell, S., & Stein, T. (2026). Wearable Sensors and Machine Learning for Field-Based Biomechanical Load Assessment in Sports: A Structured Overview of Current Research. *Current Issues in Sport Science*, *11*(3), Article 005. https://doi.org/10.36950/2026.3ciss005

Introduction

The assessment and monitoring of musculoskeletal load is essential for effective athletic training and long-term health in sports (Camomilla et al., 2018). These efforts aim to identify deficiencies in movement execution, optimize performance, and reduce the risk of injury (Claudino et al., 2019). In recent years, interest in wearable approaches for assessing movement kinetics, such as ground reaction force (GRF) (Yılmazgün et al., 2025), has grown. This shift is driven by the limitations of traditional laboratory-based techniques, including optical motion capture systems and force plates, which, while accurate, are often costly, immobile, and impractical for use during training or competition (Lee & Lee, 2022).

Wearable sensors, such as inertial measurement units (IMUs), provide practical alternatives (Lee & Lee, 2022). These body-mounted devices are portable, relatively inexpensive, and non-invasive, making them well suited for field applications (Camomilla et al., 2018; Rattanakoch et al., 2023). However, converting the collected data into meaningful biomechanical metrics and interpreting the resulting large, high-dimensional time-series data presents significant analytical challenges (García-de-Villa et al., 2023; Stetter & Stein, 2024).

To address these challenges, machine learning (ML), such as artificial neural networks (ANNs), have gained increasing attention (Ferber et al., 2016; Halilaj et al., 2018; Stetter & Stein, 2024). These data-driven models can learn the relationships between wearable sensor inputs and biomechanical outputs without requiring explicit knowledge of the underlying biomechanical models (Ancillao et al., 2018; Wouda et al., 2018). This ability is particularly valuable in settings where direct biomechanical measurements are impractical or unavailable (Verheul et al., 2020; Xiang et al., 2022).

Research in sports-related ML has expanded rapidly, with no sign of declining interest (Dindorf et al., 2024; Zhou et al., 2025). Recent reviews have highlighted ML applications in athletic performance prediction and movement classification using wearable sensors (Claudino et al., 2019; Cust et al., 2019), but relatively few have focused on biomechanical load assessment in field settings in different sports. As an example, Xiang et al. (2022) reviewed ML techniques for lower limb running biomechanics but did not extend their analysis to broader sporting contexts or sensors beyond IMUs. In addition, Verheul et al. (2020) emphasized a persistent gap in field-based biomechanical load assessment, particularly at joint and tissue levels, and identified ML as a promising approach to address this challenge.

Accordingly, this review systematically summarizes the current state of research on wearable sensors and ML for field-based biomechanical load assessment across diverse sports. Specifically, it examines the sports and movement tasks studied, the types and placements of wearable sensors used, the ML approaches applied, and the biomechanical load metrics assessed.

The novelty of this review lies in its broad, cross-sport perspective. In contrast to previous work that has focused primarily on running and lower-limb biomechanics (e.g., Xiang et al., 2022), the present study considers field-based applications across a wide range of sports and do not restrict the analysis to a single sensor modality. This cross-sport, sensor-inclusive scope enables what is, to our knowledge, the first structured overview of current knowledge on wearable

sensors and machine learning for field-based biomechanical load assessment in sports. By jointly analyzing study designs, sensor types, ML approaches, and target load metrics, this review reveals cross-sport trends and methodological gaps, thereby providing a basis for transferring methods across sports and making informed choices for future research, particularly in under-represented sports.

Methods

Search strategy

The PubMed and SPORTDiscus databases were used to identify relevant studies. Initial searches were conducted on December 9th, 2023 and the search was rerun on March 7th, 2025. Relevant studies were identified using keywords reflecting four main categories (Table 1): wearable sensors, machine learning, biomechanical load metrics, and sports.

Table 1
Boolean Search Strategy to Identify Relevant Studies.

Category	Search terms
Wearable sensors	("field based" OR "in the field" OR "in field" OR "field-based" OR field OR "wearable sensor" OR wearable* OR portable OR worn OR cloth* OR "body mounted" OR mobile OR IMU OR "inertial measurement unit" OR "inertial sensor" OR "inertial motion capture" OR acceleromet* OR gyroscope* OR magnetomet* OR MARG OR "magnetic angular rate and gravity" OR electromagnetic OR EMG OR electromyography OR "electronic skin" OR insole OR "in-sole" OR “plantar pressure”)
	AND
Machine learning	("machine learning" OR "deep learning" OR "supervised learning" OR "unsupervised learning" OR "semi-supervised learning" OR "reinforcement learning" OR "support vector machine" OR "random forests" OR "bayesian learning" OR "decision tree" OR "artificial neural network" OR "artificial intelligence" OR "neural network" OR SVM OR AI OR ANN OR CNN OR RNN OR "convolutional neural network" OR LSTM OR "long short-term memory" OR clustering OR “k-means clustering”)
	AND
Biomechanical load metrics	(kinetic* OR load* OR moment* OR torque* OR force*)
	AND
Sports	(basketball OR gymnastic* OR skiing OR archery OR swim* OR athletics OR badminton OR baseball OR handball OR volleyball OR biathlon OR bobsleigh OR boxing OR breaking OR Canoe* OR cricket OR curling OR cycl* OR diving OR equestrian OR fencing OR skat OR football OR futsal OR golf OR hockey OR judo OR karate OR lacrosse OR luge OR "modern pentathlon" OR "nordic combined" OR rowing OR rugby OR sail* OR shoot* OR skateboard* OR skeleton OR snowboard* OR climb* OR squash OR surf* OR tennis OR "table tennis" OR taekwondo OR trampoline OR triathlon OR "water polo" OR weightlifting OR wrestling OR running OR biking OR bicycl* OR bmx OR soccer OR athlete* OR sport* OR training OR exercise)
	NOT pathology NOT animals NOT “physical activity”

The asterisk (*) after the initial letters expands the search to include all terms beginning with those letters. Quotation marks (" ") specify that the words must appear together in the exact order.

The search string was formulated using Boolean operators by combining search terms with "OR", each representing one of the main categories, to ensure that at least one of the terms was included. The sub-terms were joined with "AND" to cover the four main categories, and the operator "NOT" to completely exclude certain aspects from the search. The search in PubMed was carried out in the "All fields" area and in SPORTDiscus via the provider EBSCO in the standard setting. The studies identified were placed into EndNote 20 (Clarivate) to remove duplicates and to perform screening.

Eligibility Criteria

The search was limited to English-language articles, and review papers were excluded. The search terms were designed to exclude studies that focused on medical conditions, animal participants, or general physical activity unrelated to sport-specific contexts. This list also served to quantify the diversity of sports represented in the included studies. Studies that only assessed gait were excluded; however, studies in which gait was one of several movement tasks were included. The criterion for wearable sensor usage was considered met if the measurement technology used as input for the ML model was worn on the participant's body. Load metrics were restricted to biomechanical quantities only. In addition to metrics directly specified in our search terms, we also report related metrics (e.g., joint angles) that emerged within the included studies to provide a clearer contextual representation of load metrics (Figure 5). Physiological aspects of training load, such as metabolic performance, oxygen uptake, cardiovascular demand, or perceived exertion (Vanrenterghem et al., 2017), were excluded.

Data Extraction

Data were extracted on the methodological characteristics of each study and summarized in tabular form. Extracted information included the type of sport examined, the specific movement tasks analyzed, and participant characteristics such as age, gender, and performance level relevant to the sport. Details of the wearable sensors were also recorded, including sampling frequency, the number of sensors used, and their placement on the body. Information on the ML methods was also extracted, covering key aspects of model architecture.

A separate table summarizes the input data used for ML model training and evaluation, the corresponding biomechanical outputs, and the systems employed to provide ground truth references, used for both the ML model building and performance evaluation. This table also includes the proportions of training and test datasets, the evaluation metrics applied, and the main findings reported in each study.

Results

Search Results

The search is presented in Figure 1. A total of 5,426 articles were identified, of which 5,218 were in PubMed and 208 in SPORTDiscus. The removal of duplicates left 5,346 articles, which were supplemented by Hernandez et al. (2021), found in the reference list of the study by Xiang et al. (2023). After screening the titles and abstracts, 112 studies remained that were subject to full-text screening. This led to the exclusion of 70 studies, for reasons such as no ML or wearable sensors used, no biomechanical load metrics considered, the movement task did not meet the inclusion criteria, or cadavers were investigated. A final total of 42 studies were included.

Participant Characteristics

Nineteen studies included both women and men in comparable proportions, while 16 studies focused exclusively on male participants and six studies exclusively examined female participants. One study did not specify gender (Table 2). The mean age of participants ranged from 13.2 ± 0.5 to 35.9 ± 9.2 years. Sample sizes varied widely, from 1-133 participants, with nine studies comprising fewer than 10 participants. The mean sample size was 26 ± 27 participants.

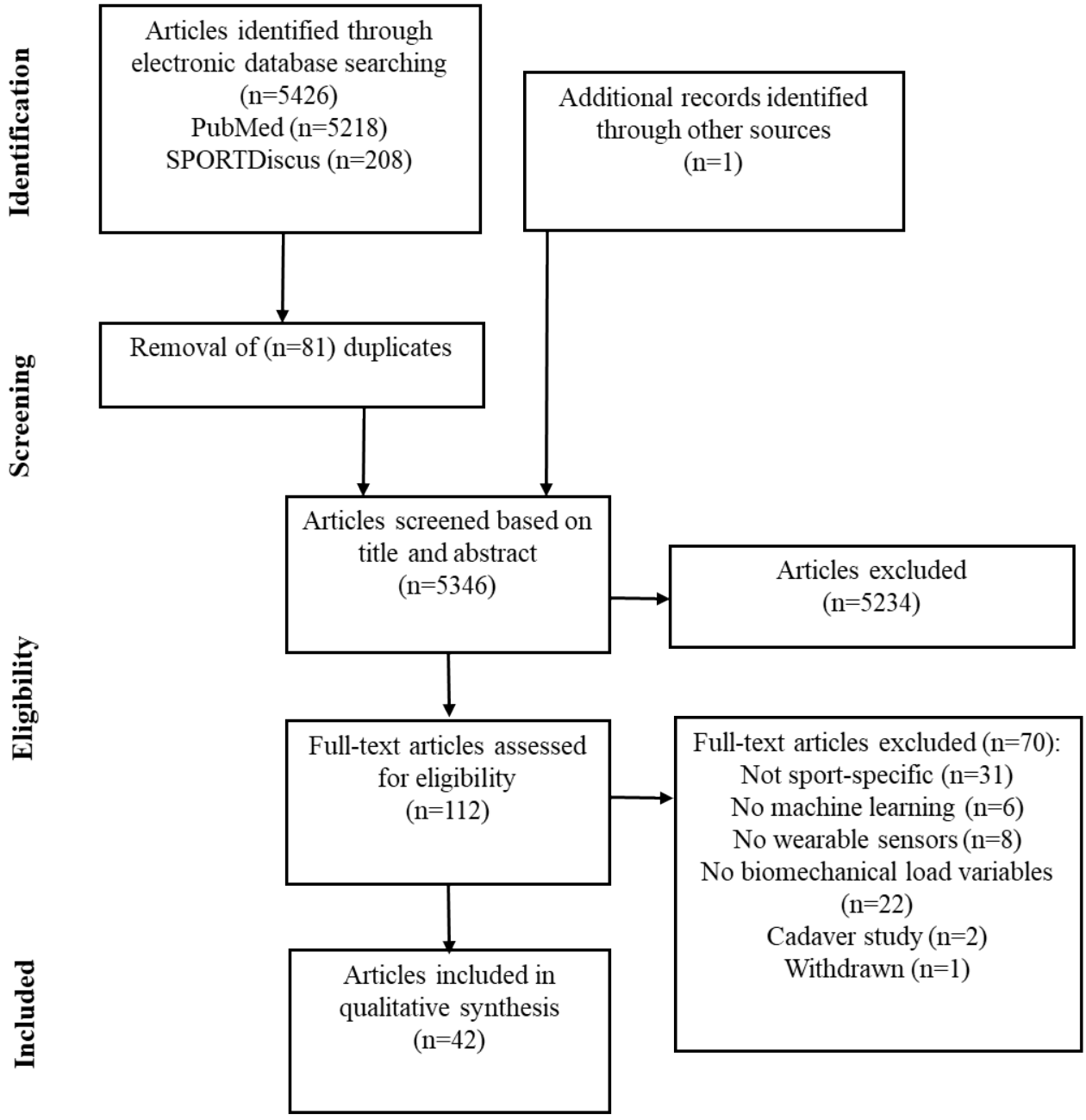

Figure 1 *PRISMA (Preferred Reporting Items for Systematic Reviews and Meta-Analyses) Flow Diagram Detailing the Article Selection Process.*

Eleven studies did not specify the performance level of the participants in relation to the sport examined. In 21 studies, participants engaged in the sport as part of university activities or during their leisure time. Furthermore, four studies intentionally included participants with diverse levels of experience (Bogaert et al., 2024; Hendry et al., 2020; Joo et al., 2016; Krumm et al., 2021).

Investigated Sports and Movement Tasks

Running was the most frequently investigated sport, featured in 24 studies (Figure 2). This was followed

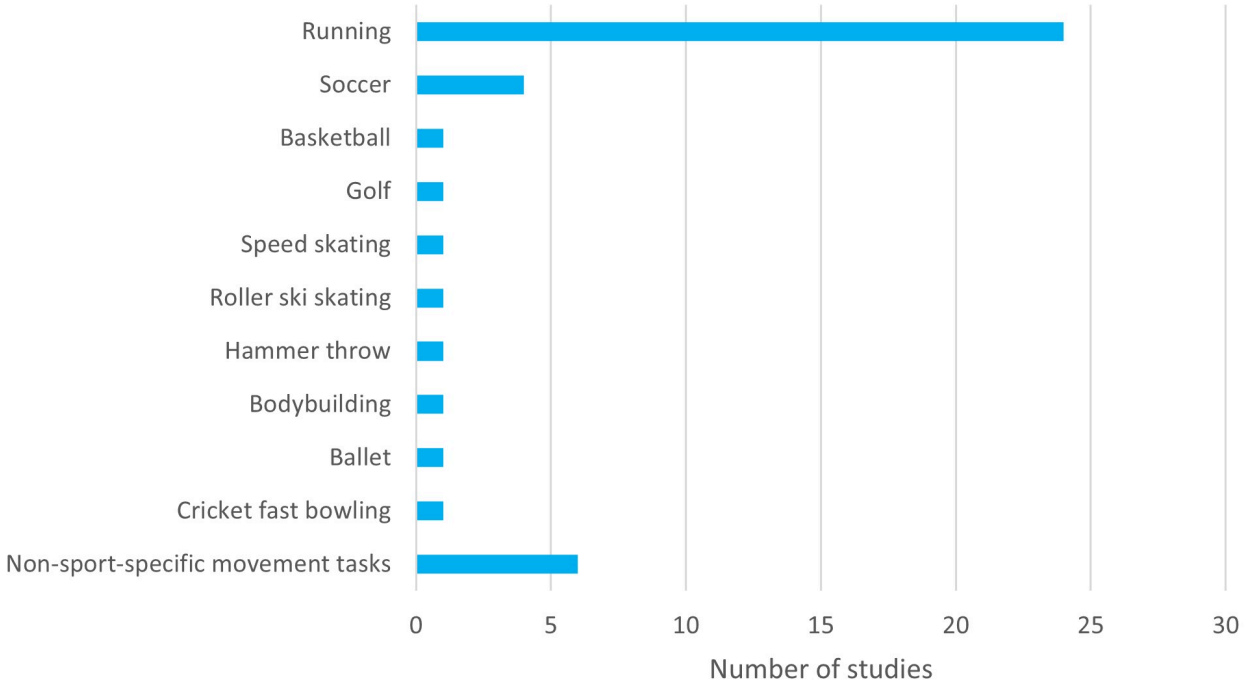

Figure 2 *The Number of Studies of Each Sport or Movement Task.*

by sport-unspecific movement tasks, examined in six studies, which included typical movements found in game sports, such as cutting maneuvers, turning movements, and jumps. Soccer was the focus of four studies. Eight other sports were each examined in a single study.

Wearable Sensor Types and Locations

IMUs were the most commonly used wearable sensors, appearing in 25 studies, followed by plantar pressure insoles (11 studies), surface EMG (3 studies), and GPS devices (3 studies) (Figure 3). IMUs were most frequently placed on the lower leg, followed by the foot, thigh, sacrum, and pelvis. EMG electrodes were applied to the thighs and/or shanks (Figure 3).

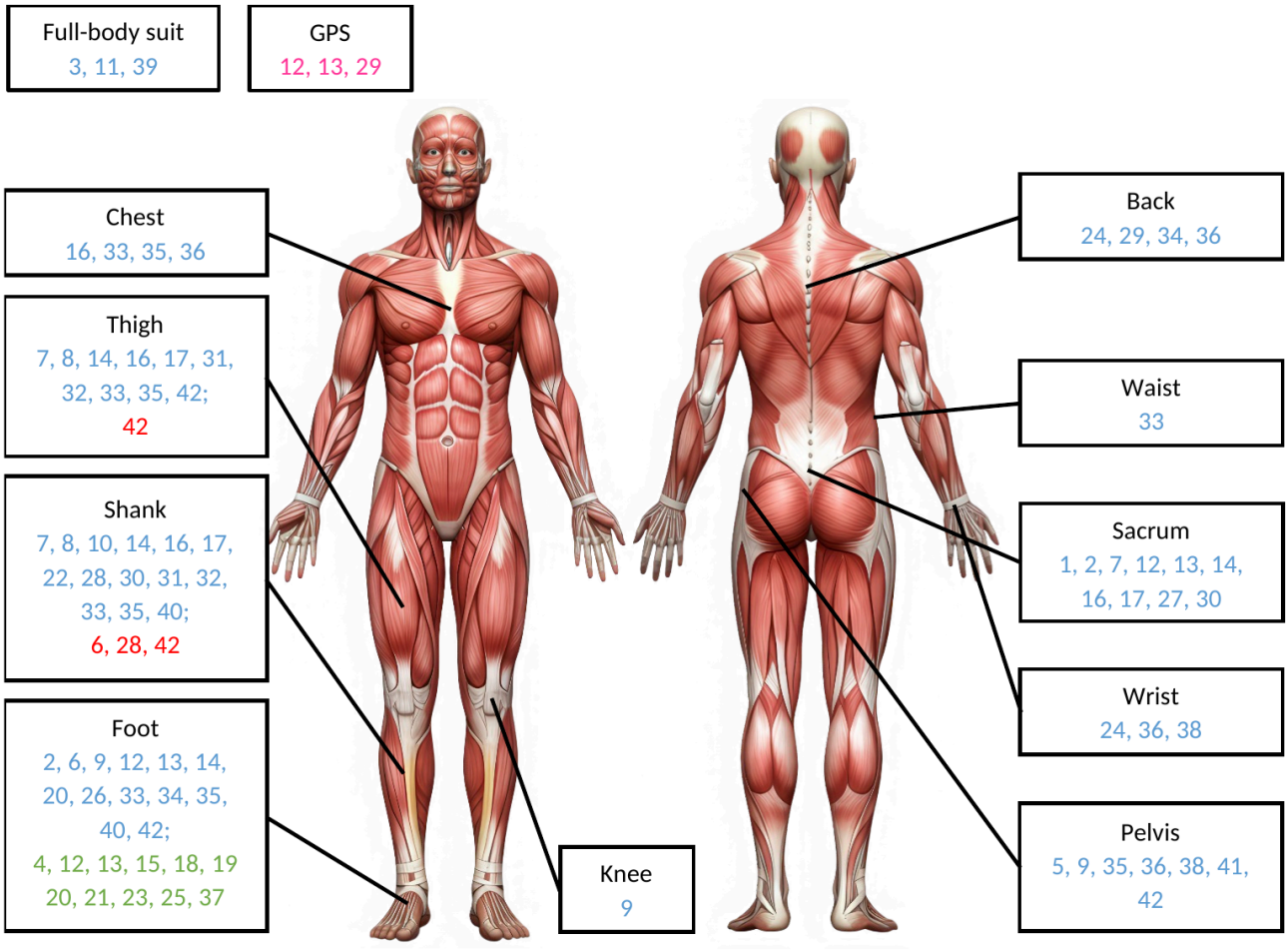

Figure 3 *Wearable Sensor Types and Locations Used in the Investigated Studies (IMU: blue; plantar pressure insoles: green; EMG: red; GPS: pink).*

The numbers refer to the studies listed in Table 2 and Table 3. Image rights obtained. © ayesha - AdobeStock

Table 2
Participants, Sports, and Wearable Sensor Specifications.

Nr.	References	Participants (female/ male)	Age (years)	Participant characteristics	Sports	Movement tasks	Number of sensors	Sensor type	Sensor locations
1	Alcantara et al. (2021)	37 (24/13)	20 ± 2	Healthy student cross-country runners	Running	Treadmill running at 3.8, 4.1 and 5.4 m/s (males) and 3.8 and 4.9 m/s (females)	1	3D-accelerometer	Sacrum on a waistband
2	Alcantara et al. (2022)	19 (9/10)	29 ± 9	NR	Running	30 x 30s running: • 3 different gradients (0°, ±5°, ±10°) • 3 speeds (2.5, 3.33, 4.17 m/s) • 3 step frequencies (preferred and ±10%) at 3.33 m/s for each gradient	3	2D-accelerometer	Sacrum, two on the right shoe only for foot strike pattern detection
3	Benjaminse et al. (2024)	32 (32/0)	15 ± 1	Talented soccer players from a regional talent training program	Soccer	Unanticipated sidestep cutting movements (40–50° change in direction)	17	3D-IMUs	Full-body
4	Billing et al. (2006)	4 (1/3)	19-27	Professional middle-distance runners in the national top 10 ranking	Running	Distance of 60m at speeds of 5-7 m/s (personal average speed in competition)	4 in one sole	Plantar pressure insoles	Left foot
5	Bogaert et al. (2024)	33 (12/31)	NR	Runners with varying experience and sports engagement	Walking and running	Treadmill running at 2.22, 2.50, 2.78, 3.33 m/s, self-reported preferred speed for a 5,000 m run, preferred speed−0.14 m/s, preferred speed +0.14 m/s	1	3D-accelerometer	Pelvis
6	(Bolus et al., 2021)	12 (4/8M)	25 ± 3	Healthy people	NR	Standing still, standing on tiptoes (two legs and one leg), calf raises with 2 s per cycle (two legs and one leg), level	1/5	1D-accelerometer/ EMG	Above the left Achilles tendon / on the

Nr.	References	Participants (female/ male)	Age (years)	Participant characteristics	Sports	Movement tasks	Number of sensors	Sensor type	Sensor locations
						walking on treadmill (1.0, 1.3, 1.6 and 1.8 m/s), level running on treadmill (2.0, 2.3 and 2.6 m/s)			left calf, on the left shin
7	Cerfoglio et al. (2021)	11 (5/6)	23 – 29	Healthy amateur athletes and people with an active lifestyle	NR	10 maximum vertical drop jumps (30 cm box height)	3	3D-IMUs	Sacrum, thigh, lower leg
8	Chaaban et al. (2021)	25 (25/0)	20 ± 1	Healthy people with moderate physical activity at least 3 x 30 min per week	NR	8 forward jump landings from a 30 cm high box (max. vertical jump immediately after landing)	4	IMUs (2D-accelerometer)	Right and left upper and lower legs
9	Chen et al. (2025)	12 (0/12)	23 ± 1	Runners with no recent history of lower-limb injuries	Running	Running at five different speeds (8, 10, 12, 14 and 16 km/h)	4	3D-IMUs	Hip, knee, ankle and foot
10	Derie et al. (2020)	93 (38/55)	35 ± 11 (female), 36 ± 9 (male)	Healthy people with a minimum running distance of 15km/week	Running	13 rearfoot runners running a distance of 30m with speeds of 2.55 m/s, 3.20 m/s, 5.10 m/s and preferred running speed 80 people running with any foot strike pattern) a distance of 30m at 3.20 m/s	2	3D-accelerometer	Left and right shin
11	Di Paolo et al. (2023)	24 (24/0)	15 ± 1	Talented female soccer players	Soccer	Laboratory task: 5m run-up, then one-footed landing with dominant leg and change of direction of 40-45°, then run through a goal 5m away Field tasks (during training sessions): • Exercises: soccer-specific elements such as	17	3D-IMUs	Full-body

Nr.	References	Participants (female/ male)	Age (years)	Participant characteristics	Sports	Movement tasks	Number of sensors	Sensor type	Sensor locations
						one-/two-legged jumps, landing, running, cutting, braking, passing; each also with the ball and opponents • Game: 11:11 training game at the end of the session			
12	Donahue & Hahn (2023a)	16 (8/8), exclusion of 3 participants due to GPS problems	23	NR	Running	5 mile run on the University campus and surrounding parks	3/2 /1	3D- IMUs/ plantar pressure insoles/ GPS-watch	Back of each foot, sacrum / one per foot / on the wrist
13	Donahue & Hahn (2023b)	15 (6/9)	24	NR	Running	4 or 5 speeds over a distance of 400m (fastest pace optional; speed range 2.33-5.36m/s based on 5km pace of participants)	3/2/1	3D- IMUs/ plantar pressure insoles/ GPS-watch	Back of each foot, sacrum / one per foot / on the wrist
14	Dorschky et al. (2020)	10 (0/10)	27 ± 3	NR	NR	10 attempts each: • Walking at 0.9-1.0, 1.2-1.4, 1.8-2.0 m/s • Running at 3.1-3.3, 3.9-4.1, 4.7-4.9 m/s	7	3D-IMUs	Lower back, right thigh, lower leg and right foot
15	Hajizadeh et al. (2023)	16 (7/9)	25 ± 3	NR	Walking and running	Two test sessions one week apart: • ten walking and five jogging trials at a self-selected pace	2	Plantar pressure insoles	One per foot
16	Hendry et al. (2020)	23 (23/0)	19 ± 2	Healthy dancers with recreational and pre-	Ballet	• Unilateral jumps (repeated for both legs) • Bilateral jumps	6	3D-IMUs	Thoracic spine, sacrum, and left and

Nr.	References	Participants (female/ male)	Age (years)	Participant characteristics	Sports	Movement tasks	Number of sensors	Sensor type	Sensor locations
				professional level					right thigh and shank
17	Hernandez et al. (2021)	27 (0/27)	27 ± 4	NR	Walking and running	Treadmill walking and running starting at 4 km/h with a constant increase of 0.16 km/h every 2 seconds until the target speed: • Walking at 4 and 6 km/h • Running at 8, 10, 12 and 14 km/h	5	IMUs (1D-accelerometer)	Sacrum and both upper and lower legs
18	Honert et al. (2022)	18 (9/9)	28 ± 5	Recreational runners	Walking and running	Treadmill walking and running: • +6° at 2.6, 2.8 and 3.0 m/s • 0° at 2.6, 3.0, 3.4 and 3.8 m/s • -6° at 2.6, 2.8, 3.0 and 3.4 m/s	2	Plantar pressure insoles	One per foot
19	Joo et al. (2016)	80 (39/41)	28 ± 7	Professional and amateur golfers	Golf	Five golf swing movements	99 sensors per insole	Plantar pressure insoles	One per foot
20	Krumm et al. (2021)	7 (1/6)	34 ± 11	Speed skaters with different experience levels	Speed skating	Speed skating imitation exercises on slide board (five complete push-off phases per leg)	2/8 sensors per insole	3D-accelerometer/ plantar pressure insoles	Both ankles/ one per foot
21	Lang et al. (2025)	9 (2/7)	23 ± 2	Healthy people	Running (in-place)	Alternately lifting the legs following an audio file with a moderate, steady “one-two, one-two” to simulate running in place	2 insoles, 8 sensors per insole	Plantar pressure insoles	One per foot

Nr.	References	Participants (female/ male)	Age (years)	Participant characteristics	Sports	Movement tasks	Number of sensors	Sensor type	Sensor locations
22	Long et al. (2024)	4 (0/4)	21 ± 2	Healthy collegiate basketball players	Basketball	Various basketball-specific tasks: walking, jogging, running, sidestep cutting, max-height jumping, stop-jumping	1	IMU	Right distal medial tibia
23	Lozano-Berges et al. (2019)	40 (0/40)	13 ± 1	Soccer players	Soccer	Soccer-specific tasks: two-legged jumps over 30cm hurdles, zigzag run around four poles, sideways sprint, sprints with 90° cutting maneuver, maximum sprints	64 sensors per insole	Plantar pressure insoles	One per foot
24	McGrath et al. (2023)	18 (0/18)	19 ± 1	Sub-elite cricket fast bowlers	Cricket fast bowling	36 throws from the line, 12 throws per intensity zone: low = 70%, medium = 85%, high = 100% of the maximum perceived bowling effort	2	IMUs (each with a different accelerometer)	T1 vertebra and on the bowling wrist
25	Moore et al. (2020)	30 (0/30)	34 ± 7	Recreational runners	Running	Running at a comfortable speed (2.7 ± 0.4 m/s) over a straight 5 m course with 6 different foot strike pattern types: natural, extreme-forefoot, forefoot, midfoot, rearfoot, extreme-rearfoot	2	Plantar pressure insoles	One per foot
26	Ngoh et al. (2018)	7 (0/7)	21 ± 1	NR	Running	Treadmill walking at 4 km/h and running at 8, 9 and 10 km/h	1	IMU (1D-accelerometer)	Centrally on top of the right shoe
27	(Patoz et al., 2023)	100 (27/73)	29 ± 7 (female), 30 ± 8 (male)	Recreational runners	Running	Treadmill running in random order at 9, 11, 13 km/h	1	IMU	Sacrum
28	Play et al. (2024)	133 (56/77)	18 – 65	Recreational runners	Running	8.5-min running at self-selected speed	1/1	EMG/3D-accelerometer	Gastrocnemius medialis
29	Pogson et al. (2020)	15 (5/10)	23 ± 1	Running team athletes	Running	Accelerating, decelerating and constant running tests on flat	1	3D-accelerometer with GPS	Back

Nr.	References	Participants (female/ male)	Age (years)	Participant characteristics	Sports	Movement tasks	Number of sensors	Sensor type	Sensor locations
						ground: 2 to 8 m/s with increments of 1 m/s			
30	Song et al. (2025)	44 (25/19)	NR	Competitive collegiate distance runners	Running	Treadmill running at multiple speeds with at least 60 steps (approximately 15 seconds): females at 3.8 and 4.9 m/s, males at 3.8, 4.1 and 5.4 m/s	3	3D-IMUs	Sacrum, left shank and right shank
31	Stetter et al. (2020)	13 (0/13)	26 ± 3	Healthy sports students	NR	6 tasks at self-selected speed: walking straight, 90° walking turn, moderate running, fast running, 90° running turn, 45° cutting maneuver	2	3D-IMUs	Integrated into the knee sleeve (thigh and shank)
32	Stetter et al. (2019)	13 (0/13)	26 ± 3	Healthy sports students	NR	Sports-specific tasks: moderate running, fast running, 90° turns, sprint start, full stop after sprint, left/right cutting maneuver, lateral shuffle cut, walking, walking 90° turns, single-legged horizontal jumps, two-legged vertical jumps	2	3D-IMUs	Integrated into the knee sleeve (thigh and shank)
33	Sun et al. (2023)	16 (0/16)	23 ± 1	Healthy people	NR	30 two-legged and 15 one-legged drop landing tasks from 30 cm height	8	3D-IMUs	Chest, waist, upper and lower legs and feet
34	Tan et al. (2022)	16 (7/9)	23 ± 2	Healthy recreational runners	Running	Running in four conditions in randomized order: two types of shoes (minimalist and standard shoes, 2.4 and 2.8 m/s, each with 100 steps each with forefoot, midfoot and rearfoot striking patterns	1	IMU	Back of the left shoe
35	Tan et al. (2021)	15 (7/8)	24 ± 1	Healthy recreational runners	Running	Running in four conditions in randomized order: two types	1 to 5	IMUs (3D-accelerometer)	Chest, pelvis, left thigh and

Nr.	References	Participants (female/ male)	Age (years)	Participant characteristics	Sports	Movement tasks	Number of sensors	Sensor type	Sensor locations
						of shoes (minimalist and standard shoes, 2.4 and 2.8 m/s, each with 100 steps each with forefoot, midfoot and rearfoot striking patterns			lower leg and left foot
36	Uddin et al. (2021)	13 (0/13)	25 ± 3	Healthy professional skiers	Roller Ski Skating	Roller ski skating with elite roller skis on a treadmill on two consecutive test days: Day 1: 12 submaximal units of 4 minutes each at a constant speed and three different subtechniques with four different intensities (inclinations & speeds), then a maximum step test until exhaustion Day 2: two 21-minute stages (first low intensity, then at competition intensity) with freely chosen technique over terrain profile, then immediately step-by-step all-out test until exhaustion	7	IMUs (3D-accelerometer)	Upper back, chest, lower back, both wrists and both ski bindings
37	Van Hooren et al. (2024)	19 (0/19)	24 ± 4	Runners free of musculoskeletal injuries	Running	Treadmill running at 2.78, 3.00, 3,33, 4.00, 5 m/s, four slopes (-6°, -3°, 0°, 3°, 6°), with different step frequencies (lower, higher), and forward trunk lean	2	Plantar pressure insoles	One per foot
38	(Wang et al., 2022)	1 (0/1)	NR	University athletes	Hammer Throw	Hammer throws	2/1	IMUs/Load cell	Wrist, hip/ hammer handle
39	Wouda et al. (2018)	8 (0/8)	25 ± 5	Healthy experienced runners	Running	Treadmill running at 10, 12, 14 km/h	17	3D-IMUs	Full-body

Nr.	References	Participants (female/ male)	Age (years)	Participant characteristics	Sports	Movement tasks	Number of sensors	Sensor type	Sensor locations
40	Xiang et al. (2023)	32	26 ± 3	Recreational runners	Running	10 km run at 11.2 ± 1.2 km/h, before and after determining the foot posture index	4	3D-IMUs	Dorsum of the right foot and on the antero-medial tibia
41	Zago et al. (2019)	13 (13/0)	24 ± 3	Soccer players from elite clubs in the first and second leagues of Italy	Soccer	5m shuttle run test at average speed of 70% of the respective maximum aerobic speed (2.5 ± 0.2 m/s) until exhaustion	1	IMU (3D-accelerometer)	Pelvic
42	Zangene et al. (2021)	19 (0/19)	25 ± 5	Healthy and well-trained bodybuilders	Bodybuilding	5 squats each without load, then with 60%, 80% and 100% of the personal 5RM (maximum execution of 5 repetitions)	8/5	IMUs/EMGs	Feet and thighs and on the pelvis/ front and back thigh, calf and shin of the right leg

NR: not reported in the study.

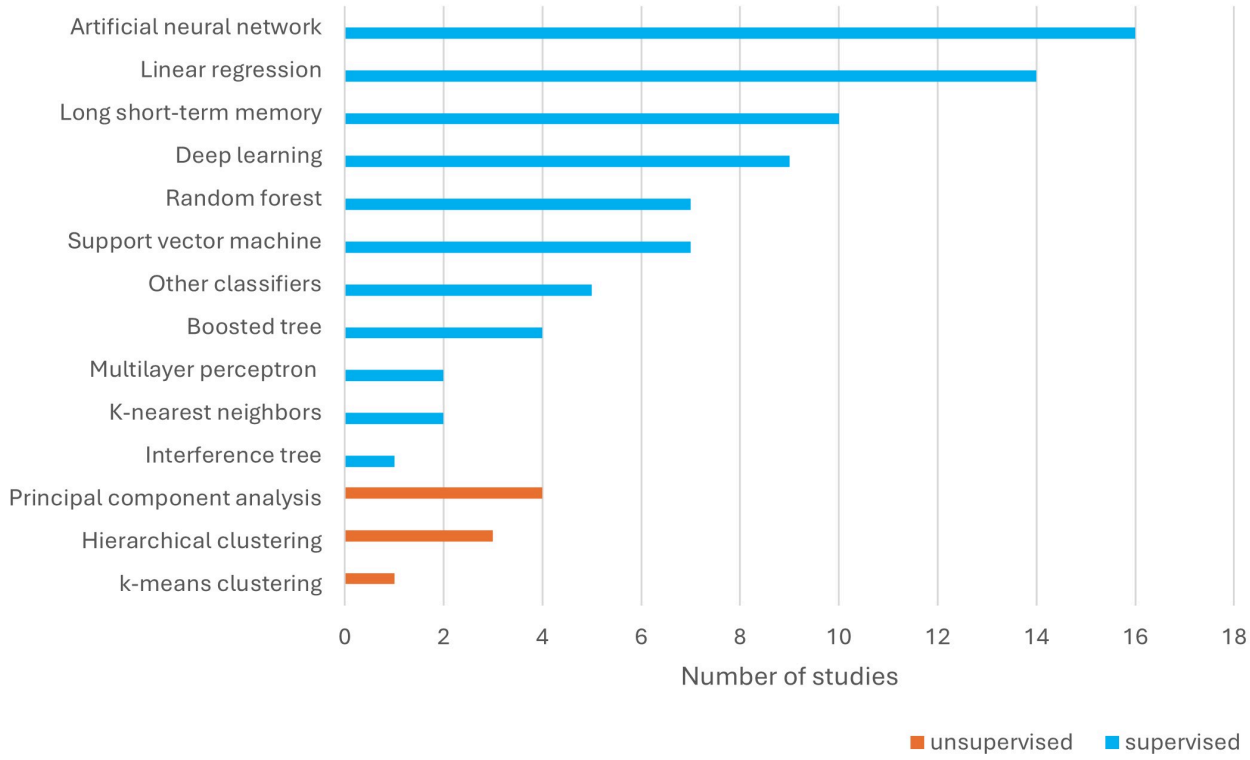

Figure 4 *The Number of Studies for Each Machine Learning Approach.*

Blue bars represent supervised machine learning approaches, while orange bars show unsupervised machine learning approaches.

ML Approaches

The most commonly-used ML approaches were ANNs (16 studies), followed by linear regression (14 studies) and long short-term memory networks (10 studies) (Figure 4, Table 3). In nine studies a deep learning approach was used. Random forest and support vector machines were used in seven studies each. Among unsupervised ML, principal component analysis (PCA), hierarchical clustering, and k-means clustering were used in four, three, and one study, respectively.

Biomechanical Load Metrics

Biomechanical load was most frequently investigated by GRF metrics (29 studies; Figure 5, Table 3). Movement execution metrics were the next most commonly analyzed variables, appearing in 10 studies, followed by joint moment metrics, investigated in nine studies (Figure 5, Table 3). In addition, joint angle, joint force, mechanical performance and EMG metrics were examined (Figure 5, Table 3).

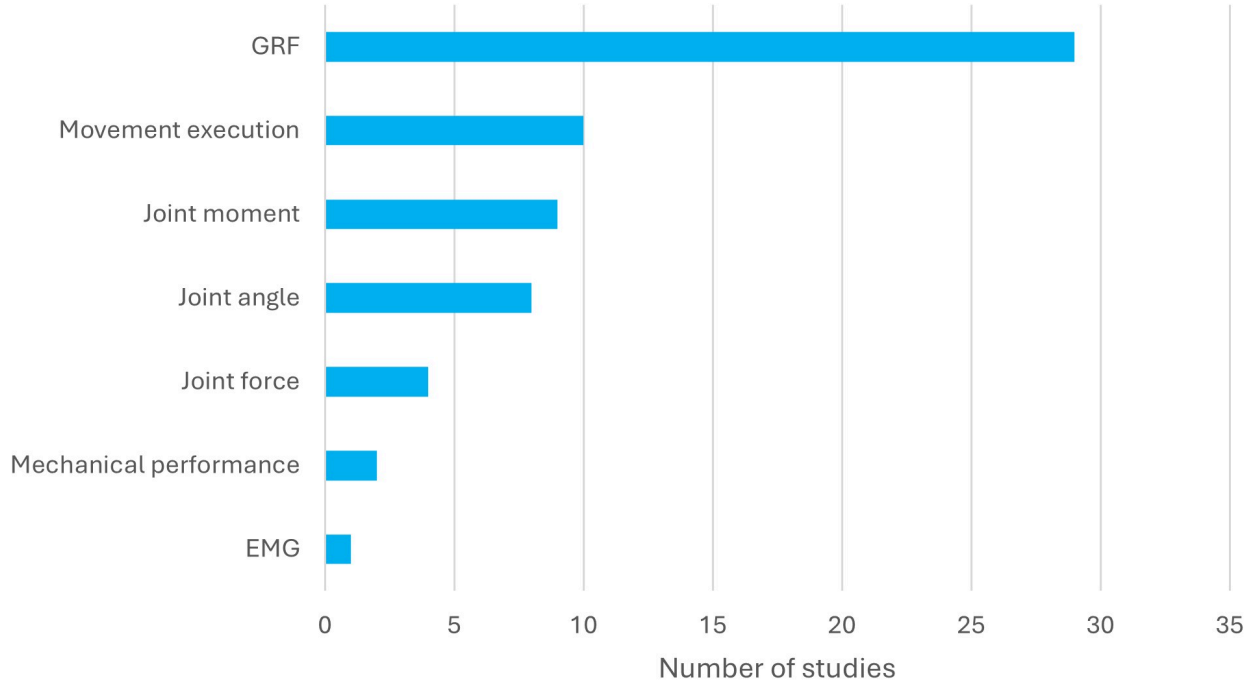

Figure 5 *The Number of Studies for the Different Categories of Biomechanical Load Metrics.*

Examples for the categories are: GRF metrics: loading rate, movement execution metrics: contact time, joint moment metrics: ankle moment, joint angle metrics: knee flexion angle, joint force metrics: knee joint force, mechanical performance metrics: mechanical power, EMG metrics: sum of calf EMG magnitude. GRF: ground reaction force; EMG: electromyography.

Table 3
The Detailed Machine Learning (ML) Approaches and Key Findings of the Studies.

Nr.	Reference	ML approach	Input	Dataset split	Validation	Biomechanical output	Evaluation	Reference data	Key findings
1	Alcantara et al. (2021)	• Quantile regression forests (QRF, random forest) • Linear regression (LR)	Acceleration data, running speed, stride frequency, body mass	Training/test: 19/9 participants	5-fold cross validation (CV)	• Maximum vertical GRF • Vertical impulse • Contact time	• RMSE, MAPE, r • paired t-test (α = 0.05), MAPE for comparison of models	GRF from force-measuring treadmill	• No significant differences between the MAPE of the QRF and LR model prediction for maximum vertical GRF (p = 0.549) and vertical impulse (p = 0.073) • MAPE of the LR model lower than for the QRF model (p= 0.049) • QRF and LR model can predict maximum vertical GRF, vertical impulse and contact time with accuracy of MAPE < 5%
2	Alcantara et al. (2022)	Long short-term-memory (LSTM) network	Vertical and anterior-posterior acceleration data (in overlapping windows of 12 ms) Feature engineering: body mass; height; running speed; slope; percentage of strides as back, mid or forefoot steps; mean, stan-	Test-train split divided by gradient based on data from participant 14 (±5° trials are reserved for testing, 0° and ±10° gradients are for training)	Leave-one-subject-out cross-validation (LOSOCV)	Continuous GRF-waveforms (perpendicular to the surface)	RMSE, rRMSE, MAPE	GRF from force-measuring treadmill	• Average RMSE = 0.16 ± 0.04 body weight (BW) and relative RMSE= 6.4 ± 1.5% • Prediction of continuous normal GRF waveforms with greater accuracy than presented in previous studies

Nr.	Reference	ML approach	Input	Dataset split	Validation	Biomechanical output	Evaluation	Reference data	Key findings
			dard deviation and range of acceleration data for each window						
3	Benjaminse et al. (2024)	32 classification models: 6 support vector machines (SVM), 6 nearest neighbor classifiers, 5 ensemble classifiers, 5 neural network classifiers, 3 decision trees, 2 discriminant analysis, 2 naïve bayes classifiers, 2 kernel approximation classifiers, 1 logistic regression classifier; PCA for dimensionality reduction	Knee, hip, ankle, and pelvis joint kinematics: mean and peak angle over 0–20% of the stance phase, angle at the peak knee abduction moment (KAM)	Training/test: 80%/20% of the total dataset	5-fold CV	• Classification: high and low knee abduction moments (KAMs) • Regression: KAM values	Area under curve (AUC), true positive rate (TPR), and positive predictive values (PPVs)	Motion capture system, force plates; Vicon Plug-in-Gait lower body model	Classifying high versus low KAMs during agility with good approximation (AUC 0.81 – 0.85) represents a step towards testing in an ecologically valid environment
4	Billing et al. (2006)	ANN, multilayer regression (MLR)	Force values of the insoles (scaled between 0 and 1)	Training/test: 6 attempts/ three attempts of one participant		Vertical, anterior-posterior and medio-lateral components of the GRF	Mean absolute error (MAE), r, average accuracy in %	Two force plates	• Vertical GRF was most accurately predicted (MLR: r = 0.999, ANN: r = 0.997), followed by anterior-posterior (MLR: r = 0.979, ANN: r = 0.980) and medio-lateral (MLR: r = 0.896, ANN: r = 0.858) • MLR was the most accurate predictor of vertical (r = 0.999, MAE = 33.411 N) and medio-lateral (r

Nr.	Reference	ML approach	Input	Dataset split	Validation	Biomechanical output	Evaluation	Reference data	Key findings
									= 0.896, MAE = 29.375 N) • ANN was slightly more accurate for the anterior-posterior component (r = 0.980, MAE = 24.321 N)
5	Bogaert et al. (2024)	Mean regressor (a model that always predicts the mean value of the target variable as computed on the training data)	Acceleration data; Features divided into three categories: participant-specific features include mass and leg length, general time-series features, domain-specific time-series features include step frequency, impulse of vertical acceleration data during the stance phase, and impulse of the entire step of the vertical acceleration data	Training/test: 36/7 participants	LOSOCV	Contact time, active peak, impact peak and impulse of the vertical GRF	RMSE, MAPE, R^2	GRF from force-measuring treadmill	• active peak: RMSE = 0.080 BW, impact peak: RMSE = 0.198 BW, impulse: RMSE = 0.0073 BW · seconds, and contact time: RMSE = 0.0101 seconds • Results indicate the potential utility of this approach as a valuable tool for monitoring selected factors related to running-related injuries
6	Bolus et al. (2021)	Various regression models: linear regression, regression trees, support vector machines with various kernel functions	Acceleration signal segmented into individual vibration windows 70 features: temporal and amplitude-	NR	LOSOCV; selection of the best model by 10-fold CV	Net ankle moment, sum of calf EMG magnitude	R^2 and RMSE	Motion capture system, GRF from force-measuring treadmill, three EMG electrodes; Vicon Plug-in-Gait lower body model	Net ankle moment (captures general tendon tension trends) across running speeds and participants: R^2 = 0.82 ± 0.19, RMSE = 0.73 ± 0.39 $\frac{Nm}{kg}$

Nr.	Reference	ML approach	Input	Dataset split	Validation	Biomechanical output	Evaluation	Reference data	Key findings
			based attributes of the tendon response profile (e.g. rise and fall time, peak/median amplitude)						
7	Cerfoglio et al. (2021)	ANN	3D acceleration and 3D angular velocity signals of the three IMUs	Training/test: 7/4 participants	20-fold CV	3D GRF, 3D knee moments	RMSE	Motion capture system, two force plates; Visual 3D model	• Time course of GRF: mean RMSE= 0.02 $\frac{Nm}{kg}$ • 3D knee joint moments: mean RMSE = 0.4 $\frac{Nm}{kg}$
8	Chaaban et al. (2021)	• Single feature model: simple linear regression • Multiple feature model: stepwise linear regression	Single feature model: lower leg IMU data (accelerometer and gyroscope), 113 features Multiple feature model: lower leg and thigh IMU data (acc. only), 113 features; lower leg and thigh IMU data (acc. + gyr.); 225 features	Training/test: 9 attempts/1 attempt	10-fold CV; minimizing the number of features to select the best model	Maximum vertical GRF, maximum knee flexion angle, maximum knee extension moment, maximum force absorption of the knee in the sagittal plane	RMSE, nRMSE, R^2	Motion capture system, two force plates; Visual 3D model	• Multiple feature models, especially with accelerometer and gyroscope data, valid predictors: R^2 = 0.68 – 0.94, nRMSE = 4.6% – 10.2% • Single feature models performed lower: R^2 = 0.16 – 0.60, nRMSE = 10.0% – 16.2%
9	Chen et al. (2025)	Four different deep learning models (CNN): CNN-xLSTM, CNN-sLSTM, CNN-mLSTM, CNN-LSTM	Joint angles: 3D ankle, 3D hip, 3D knee	Training/test: 9 subsets/1 subset	10-fold-CV	vGRF	R^2, MAPE, RMSE	Motion capture system, force plates; no biomechanical model information	• CNN-xLSTM consistently performed best when different datasets were input (R^2 = 0.909 ± 0.064, MAPE = 2.18 ± 0.09, RMSE = 0.061 ± 0.008)

Nr.	Reference	ML approach	Input	Dataset split	Validation	Biomechanical output	Evaluation	Reference data	Key findings
10	Derie et al. (2020)	Linear regression with elastic net regularization, linear regression with least absolute shrinkage and selection operator regularization (LASSO), gradient boosted regression trees (XGB)	3D acceleration waveforms Features from 3 categories: automatically-generated statistical features of the 3D acceleration waveforms, experiment-specific features, participant-specific features	Training/test: 1 participant, all but one attempt/1 participant, withheld attempt 93 participants/1 participant	LOSOCV	Maximum instantaneous vertical load rate	MAE and R^2, in two steps (first over all participants, then all participants with at least 10 trials); ANOVA, Cohens' d effect sizes	Two force plates	• Participant-dependent XGB model most accurate: XGB: MAE = 5.39 ± 2.04 BW/s , R^2 = 0.9461, MAPE = 6.08% • Similar participant-independent XGB model: MAE = 12.41 ± 7.90 BW/s, R^2 = 0.7741, MAPE = 11.09%
11	Di Paolo et al. (2023)	Hierarchical clustering (Ward linkage method)	3D knee, hip, ankle and pelvis joint kinematics from IMUs	NR	NR	Classification into knee joint moment clusters	One-way ANOVA by statistical parametric mapping (SPM) to compare groups (for knee, hip, ankle and pelvis respectively)	Motion capture system, two force plates; Vicon Nexus Software and Xsens MVN Analyze system for modelling	Three clusters: Cluster 1: lowest knee moments, Cluster 2: high knee extension, but low knee abduction and rotation moments, Cluster 3: highest knee abduction, extension and external rotation moments
12	Donahue & Hahn (2023a)	LSTM	IMU data of both insteps and sacrum: 3D accelerations and angular velocities, resulting acceleration and angular velocity	Training/test: 12/1 participant	LOSOCV	GRF waveforms, Calculated from GRF: contact time, standing average force, maximum force, impulse, loading rate	RMSE, linear models, bias analysis; linear regression, R^2	Plantar pressure insoles	• Accurate estimation of contact time: RMSE = 0.031s, R^2 = 0.524 • Waveform step-by-step average across all speeds and gradients: RMSE = 0.33 BW per step • GRF magnitudes generally underestimated by LSTM when data from new participants were added, especially at

Nr.	Reference	ML approach	Input	Dataset split	Validation	Biomechanical output	Evaluation	Reference data	Key findings
									higher running speeds
13	Donahue & Hahn (2023b)	LSTM	IMU data of both insteps and sacrum: 3D accelerations and angular velocities, resulting acceleration and angular velocity	Training/ test/ validation: 70%/15%/15%	LOSOCV	GRF waveform, calculated from this: contact time, standing average force, maximum force, impulse, loading rate	R^2, RMSE, linear regression	Plantar pressure insoles	• Comparable prediction accuracy of GRF waveform as previous studies: RMSE 0.189 BW – 0.288 BW • Foot contact time: RMSE 0.089 s –0.021 s, R^2= 0.795 • Estimation of kinetic variables varied, best performance in estimation of maximum force R^2 = 0.614
14	Dorschky et al. (2020)	Eight convolutional neural networks, one for each output	IMU data from the hip, right thigh and lower leg and foot sensors: acceleration in the sagittal plane (anterior-posterior and longitudinal axes) and angular velocity (medio-lateral axis)	Training/test: 7/3 participants, 4/3 participants, 2 /3 participants	LOSOCV	Right hip, knee and ankle angles and moments; Vertical and anterior-posterior GRF	RMSE R^2	Motion capture system, force plate; Individualized musculoskeletal models	• Reduction in RMSE by adding simulated IMU data: for hip, knee and ankle angles by 17%, 27% and 23%; for knee and ankle moments by up to 6%; for anterior-posterior and vertical GRF by up to 2% and 6% • Simulation-based estimation of joint moments and GRFes was limited by inaccuracies of the

Nr.	Reference	ML approach	Input	Dataset split	Validation	Biomechanical output	Evaluation	Reference data	Key findings
									biomechanical model
15	Hajizadeh et al. (2023)	Two LSTM: 1. walking 2. jogging	252 plantar foot pressure values of the insole sensors in a masked pressure matrix (pressure value determined from 4x4 neighboring sensors)	Training/test/validation: walking: 22/5/5 participants Jogging: 21/5/5 participants	MSE loss criterion	3D GRF	MAE, RMSE, nRMSE, r	Force plate	• Predictions for walking more accurate than for jogging (MAE = 5.25 ± 2.06% BW vs. MAE = 13.26 ± 4.26% BW) • Higher error and lower correlation for medio-lateral force component compared to vertical and anterior-posterior
16	Hendry et al. (2020)	SVM, two ANNs	Vector magnitude of the acceleration data	Training/test: 14/2 participants	5-fold CV, LOSOCV	Maximum GRF	RMSE, r, Bland-Altman-Plots	Force plate	Single sensor model based on sacrum data most accurate: Unilateral: RMSE = 0.24 BW, r = 0.95, bilateral: RMSE = 0.21 BW, r = 0.98
17	Hernandez et al. (2021)	Deep learning neural network with convolutional and recurrent layers	IMUs: 3 channels for acceleration and 3 channels for angular velocity	Training/test: 23/4 participants	k-fold CV with 2 loops and "early stopping" at each k-fold as soon as RMSE of the test set increases even though that of the training set decreases	Lumbar extension, flexion and rotation and 6 DOFS for each lower extremity: hip flexion, abduction and rotation, knee flexion, ankle dorsiflexion and inversion	Mean error, MAE, r	Motion capture system, OpenSim musculoskeletal model	• For the different DOFs: MAE range 2.2 ± 0.9 to 5.1 ± 2.7° with an average of 3.6 ± 2.1°, r range 0.67 ± 0.23 to 0.99 ± 0.01 • Reliable prediction without specific knowledge of the wearer's body characteristics or the position and orientation of the IMU

Nr.	Reference	ML approach	Input	Dataset split	Validation	Biomechanical output	Evaluation	Reference data	Key findings
18	Honert et al. (2022)	Linear regression and recurrent neural network; generic and participant-specific variant	Plantar pressure from five regions and three additional inputs (running speed, running slope, and subject mass)	Training/test: 17/1 participant	LOSOCV	Vertical and anterior-posterior GRF	Statistical Parametric Mapping (SPM) with two-sided paired SPM-t-test, RMSE, r	Force-measuring treadmill	• Recurrent neural network outperformed linear model in all conditions, especially in predicting anterior-posterior GRF (RNN: average error of 5.0% vs. linear model: 6.7%) • Participant-specific model: reduction of average error across all conditions, e.g. from 7.7% to 2.9% for vertical GRF
19	Joo et al. (2016)	Different wavelet neural networks with different inputs (four, five, seven or eight inputs) PCA and mutual information for dimension reduction	Uniaxial plantar foot pressure data; extended by: pressure center pattern, plantar foot pressure measurements of the other foot, pressure values integrated into the time axis	Training/test: 64/8 participants	5-fold CV	Six-axis GRF: 3 (medio-lateral, vertical, anterior-posterior) force axes and three moment (GFM) axes	RMSE, nRMSE, r	Two force plates	• Plantar pressure plus other foot (r = 0.73 – 0.97): best for vertical GRF, frontal & transverse moments (left) and AP/ML GRF, frontal GRF, transverse GRM (right). • Plantar pressure plus CoP (r = 0.83 –0.98): best for AP/ML GRF & sagittal moment (left) and vertical GRF & sagittal moment (right).
20	Krumm et al. (2021)	Deep learning neural network and multi-variable	16 plantar pressure signals and 3D acceleration	Training/test: 6 trials on day 1/remaining four trials	Minimization of RMSE output and measured	Medio-lateral push-off force time curve	RMSE, absolute differences and relative differences	Force-measuring Slide-Board with two force plates	Linear regression model sufficient to predict push-off forces: total relative difference

Nr.	Reference	ML approach	Input	Dataset split	Validation	Biomechanical output	Evaluation	Reference data	Key findings
		linear regression model	data from the two accelerometers	from day 1 and ten trials from day 2	force-time curve				between measured and modelled maximum push-off force < 5%, RSME = 33N
21	Lang et al. (2025)	Temporal convolutional network and transformer modules	Eight-channel pressure insole signals	Training/test: Entire randomly shuffled dataset divided with a 4:1 ratio	NR	Vertical GRF and tibia bone force	RMSE, nRMSE, MAE, R^2, r	Motion capture system, two force plates, OpenSim musculoskeletal model and finite element analysis (COMSOL Multiphysics)	• nRMSE of 7.33% for vertical GRF and 10.64% for tibia bone force • Offers a convenient solution for biomechanical monitoring in athletes and patients for early warning of fatigue-induced injuries
22	Long et al. (2024)	Random forest regression model	3D acceleration and 3D angular velocity data from the IMU; Number of features varies from 14 to 47 depending on the model	Training/test: 80%/20%	5-fold CV	Flexion-extension angles and moments of the knee and ankle	R^2, RMSE, Statistical Parametric Mapping (SPM) with two-sided paired t-test	Motion capture system, two force plates, OpenSim musculoskeletal model	• Flexion/extension angles: R^2 0.782 – 0.962, RMSE 2.19° – 11.58° • Flexion/extension moments: R^2 0.711 – 0.966, RMSE 0.10 Nm/kg – 0.41 Nm/kg
23	Lozano-Berges et al. (2019)	Hierarchical and k-means clustering	Plantar pressure from five regions (lateral, medial, forefoot, midfoot and hindfoot)	NR	Repeated cluster analysis with randomly selected subsamples; then calculation of the Cohen's Kappa coefficient to compare the original and subsample clusters	Classification into clusters depending on the maximum average plantar foot pressure	Independent t-tests (expressed as Cohen's d); ANCOVAs (expressed as partial η^2)	Volumetric bone mineral content, bone area and bone strength indices of the non-dominant tibia	• Classification into two groups: 15 players with high maximum average pressure (392.7 ± 68.2 kPa), 25 players with low maximum average pressure (261.0 ± 49.6 kPa) • Better total and cortical

Nr.	Reference	ML approach	Input	Dataset split	Validation	Biomechanical output	Evaluation	Reference data	Key findings
									volumetric bone mineral content and better total cross-sectional area in players with high maximum average pressure than in controls
24	McGrath et al. (2023)	Three models: random forest, linear SVM (LSVM), gradient boosting	Back or wrist IMU, depending on the model, either only acceleration data or acceleration and angular velocity data	Training/test: 17/1 participant	10-fold CV, LOSOCV	Vertical and horizontal maximum GRF, GRF impulse, loading rate	MAE, two-factor ANOVA for MAE comparison of models, MAPE, RMSE	Two force plates	Back IMU as input (vertical and horizontal axis) in 22/24 cases best results: maximum force: MAPE = 22.1% (LSVM), 24.1% (LSVM); impulse: MAPE = 16.2%, RMSE = 0.06 BWs (LSVM); load rate: MAPE = 32.6% (LSVM)
25	Moore et al. (2020)	Three models: multiple linear regression, interference tree, random forest	Plantar pressure data: two features from the first phase (first contact up to 33% of the stance phase), eight features from the entire stance phase (first contact up to 100%)	Training/test: 70%/30%	5-fold CV	Foot strike angle, classification: forefoot, midfoot, rearfoot	MSE, MAE, MAPE, R^2, accuracy in %, recall in %, precision in %	Motion capture system, force plate, Visual 3D foot model	• Prediction accuracy of foot strike angles similar for regression (RMSE = 5.16°), inference tree (RMSE = 4.85°) and random forest models (RMSE = 3.65°) • Classification performance for all models above 90%
26	Ngoh et al. (2018)	ANN (feed-forward)	Acceleration data of the foot IMU: after identifying the stance phase (first ground contact to last ground contact) scaling of the single-axis accel-	Training/test/validation: 280/ 120/230 data points	MSE	Vertical GRF	RMSE, r	Force-measuring treadmill with two force plates	• Vertical GRF with average RMSE < 0.017 BW) and r > 0.99 • Estimation of impact force and active force with average errors between 0.10

Nr.	Reference	ML approach	Input	Dataset split	Validation	Biomechanical output	Evaluation	Reference data	Key findings
			eration data to 100 data points						and 0.18 BW at different running speeds • Model can reduce the need for multiple wearable sensors
27	(Patoz et al., 2023)	Three different models: linear regression, SVM regression, ANN (two layers)	IMU acceleration data Additional features: Running speed, body mass, stride frequency	Training/test: 80%/20%	5-fold CV	Maximum vertical GRF, contact time, flight time, duty factor	RMSE, r, MAPE, Bland-Altman plots, one-way ANOVA with repeated measures	Force-measuring treadmill with two force plates	• No significant differences between MAPEs of the different ML models • Error of the ML models ⩽ 32%
28	Play et al. (2024)	Hierarchical clustering	Soft tissue vibrations (STV) using 3D accelerations	NR	NR	Functional groups (groups of runners responding similarly to different midsole hardness)	P-value for one-way repeated ANOVA	Motion capture system, force plate, Visual 3D model	• Three functional groups: soft (STV amplitude decreased for 61% of runners), medium (STV amplitude decreased for 11% of runners), hard (STV amplitude decreased for 28% of runners) • Differences between groups in terms of body fat percentage, running volume per week, foot/ground angle at initial contact, ankle plantarflexion and flight time
29	Pogson et al. (2020)	Multilayer perceptron and PCA in	Trunk acceleration data	Training/test: 7/8 participants	10 times randomized	GRF time series reconstructed from predicted:	R^2, RMSE	One force plate	• GRF time series with average R^2 around 0.9,

Nr.	Reference	ML approach	Input	Dataset split	Validation	Biomechanical output	Evaluation	Reference data	Key findings
		three different variants			train-test splits, Particle Swarm Optimization (PSO)	maximum, loading rate, impulse			which compares favorably to other approaches that use additional sensors • for impact maximum R^2 across activities 0.74
30	Song et al. (2025)	Three different models: Singular value decomposition (SVD) embedding regression, k-nearest neighbors regression (KNN), LSTM	Different IMU signal inputs	Training/test: 34/10 participants	k-fold CV	3D GRF time series	RMSE, relative RMSE, MAPE	Force-measuring treadmill	• Lightweight methods (i.e., SVD regression, KNN) can match or outperform alternatives • Personalized data reduce errors across all methods • Using acceleration, angular velocity, and all sacrum acceleration components improves performance
31	Stetter et al. (2020)	ANN (two hidden layers)	3D acceleration and 3D angular velocity data from the IMUs	Training/test: 12/1 participant	LOSOCV	Knee flexion moment (KFM) and knee adduction moment (KAM)	RMSE, rRMSE, r	Motion capture system, two force plates, full-body Dynamicus 9 model	• Strong concordance for KFM ($r \geqslant 0.69$, $rRMSE \leqslant 23.1$) for straight walking, 90° walking turn, moderate running, 90° running turn and 45° cutting maneuver • KAM from low ($r \leqslant 0.21$, $rRMSE \geqslant 33.8\%$) for cutting and fast running to high

Nr.	Reference	ML approach	Input	Dataset split	Validation	Biomechanical output	Evaluation	Reference data	Key findings
									(r = 0.71 ± 0.26, rRMSE = 22.3 ± 8.3%) for straight walking
32	Stetter et al. (2019)	ANN (two hidden layers)	3D acceleration and 3D angular velocity data from the IMUs	Training/test: 12/1 participant	LOSOCV	3D Knee joint forces (KJF)	rRMSE, r	Motion capture system, two force plates, full-body Dynamicus 9 model	• Vertical KJF: r: 0.60 – 0.94, anterior-posterior KJF: r: 0.64 – 0.90, medial-lateral KJF: r 0.25 – 0.60 • Summed vertical KJF and the maximum vertical KJF on average 5.7% ± 5.9% and 17.0% ± 13.6% respectively
33	Sun et al. (2023)	Modular real-time LSTM with four sub-deep neural networks	Segments accelerations and velocities from IMUs	Training/test: 15/1 participant	LOSOCV	Vertical GRF (vGRF) Knee extension moment (KEM)	RMSE, rRMSE, R^2, t-test to assess the influence of number & location of IMUs	Motion capture system, two force plates, Visual 3D full-body model	• Single leg drop landing: vGRF: R^2 = 0.88 ± 0.12 and KEM: R^2= 0.84 ± 0.14 • Double leg drop landing: vGRF: R^2= 0.85 ± 0.11 and KEM: R^2= 0.84 ± 0.12 • Best vGRF and KEM estimates by model with five IMUs (chest, waist and only one leg on thigh and lower leg and foot) for double-leg landings
34	Tan et al. (2022)	Convolutional neural network	3D accelerations and 3D	Training/test: 12/3 participants	LOSOCV	Impact index (pressure center relative to foot length)	RMSE, R^2, two-factor ANOVA to assess the influence of	Motion capture system, force-measuring	• Prediction of the strike index: RMSE =

Nr.	Reference	ML approach	Input	Dataset split	Validation	Biomechanical output	Evaluation	Reference data	Key findings
			angular velocities from IMU				speed and shoe, Cohen's d for effect sizes	treadmill, strike index calculation	6.9% and R^2 = 0.89 • Model robust to speed changes
35	Tan et al. (2021)	Convolutional neural network	3D accelerations and 3D angular velocities from IMU	Training/test: 14/1 participant	LOSOCV	Vertical average load rate (VALR)	r, nRMSE, MAE, Comparison of sensor locations using one-way ANOVA	Force-measuring treadmill	• VALR estimated with a lower-leg IMU showed a strong correlation (r = 0.94), higher than tibial acceleration with force plate VALR (r = 0.44 – 0.66). • IMU estimates on the foot, pelvis, trunk, and thigh achieved r = 0.91, 0.76, 0.69, and 0.65, respectively. • Adding 1 to 4 extra IMUs did not improve accuracy over the lower-leg setup
36	Uddin et al. (2021)	Time-sequential information-based deep LSTM, convolutional neural network, ANN	3D accelerations and 3D angular velocities from IMUs for feature engineering	Training/test: 12/1 participant	LOSOCV	Mechanical power	Mean-squared error (MSE), relative errors (RE)	Calculated work rate, equal to the average cycle propulsive power	• Participant-dependent approach: error of 3.5% • Participant-independent approach: error of 11.6% • LSTM provides more precise estimation than comparison models (convolutional neural network and ANN)

Nr.	Reference	ML approach	Input	Dataset split	Validation	Biomechanical output	Evaluation	Reference data	Key findings
37	Van Hooren et al. (2024)	ANN (six hidden layers)	12 predictors derived from the instrumented insole	Training/test: 90%/10%, 18/1 participant	10-fold CV, LOSOCV	Patellofemoral stress, tibial stress Achilles tendon strain	Relative percentage error, absolute percentage error, relative difference	Motion capture system, force-measuring treadmill, modified full-body musculoskeletal OpenSim model	• Overall relative percentage errors of 1.95 ± 8.40%, −7.37 ± 6.41%, and −12.8 ± 9.44% for the patellofemoral joint, tibia, and Achilles tendon impulse, respectively • Accuracy significantly changed with altered running speed, slope, or step frequency
38	(Wang et al., 2022)	Two deep neural networks (DNN): one simplified and one complete model (four deeply connected hidden layers)	Simplified model: Wrist positions, displacements and velocities from wrist IMU Full model: Wrist positions, displacements and velocities from wrist IMU, Hip positions, displacements and velocities from hip IMU	NR	MSE as a loss function	Selected joint angles on lower limbs (e.g. hip, knee, ankle)	Mean squared error (MSE), mean absolute error (MAE)	Motion capture system, load cell in the wire, full-body kinematic data	• Estimation errors for both models within an acceptable range (MAE about ±12° and ±4° respectively), showing strong correlation between limb coordination and IMU measurements
39	Wouda et al. (2018)	Two linked ANNs: first ANN for mapping the relative orientations of the lower legs to joint angles, second ANN for mapping the estimated joint angles and accel-	First ANN: Data from three IMUs placed on the pelvis and both lower legs Second ANN: estimated joint angles in com-	Training/test: 7/1 participant	Independent training and validation of the two models; participant-dependent and participant-independent	First ANN: *j*oint angles of the hips, knees and ankles Second ANN: vertical GRF	RMSE, r	Motion capture system, force-measuring treadmill, Plug-in-Gait model	• Individual models: Excellent agreement (r > 0.99) for most participants, knee RMSE flexion/extension angle with RMSE below

Nr.	Reference	ML approach	Input	Dataset split	Validation	Biomechanical output	Evaluation	Reference data	Key findings
		erations to vertical GRF	bination with vertical accelerations		training variant; LOSOCV				5°, RMSE GRF below 0.27 BW • Multiple participant model: decreased accuracy in discrete and continuous results, but still good agreement (r > 0.9)
40	Xiang et al. (2023)	Four models: convolutional neural network, SVM, gradient boosting, random forest	3D acceleration and 3D angular velocity data from IMUs For each model, three input conditions: tibia IMU only, foot IMU only, tibia and foot IMU	Training/test/validation: 60%/20%/20%	CV with 4 folds in inner loop, 5 folds in outer loop	Classification into foot posture types: neutral foot or foot pronation	Accuracy, precision, recall, F1-score, Matthew's correlation coefficient (MCC), area under curve (AUC)	Assessment using the foot posture index-6 scale (FPI-6)	• Highest accuracy with gradient boosting classifier with dorsal foot data as input: accuracy and AUC: 74.7 ± 5.2% and 0.82 ± 0.07 (participant-independent model) and 98 ± 0.4% and 0.99 ± 0 (participant-dependent model)
41	Zago et al. (2019)	Four models: multiple linear regression, SVM regression, boosted trees, ANN	3D acceleration and 3D angular velocity data from the sacrum IMU to derive 18 features: player load, root mean square, skewness and kurtosis of accelerations and angular velocities, altitude differences before and after the cutting maneuver	*Models 1-3:* random division into training and test *Model 4):* Training/test/validation: 70%/15%/15%	10-fold CV	• Positive and negative mechanical energy • Speed before and after turning • Direction of turning	Regression models: RMSE, MAE, R^2, Classification models: accuracy, sensitivity, specificity, AUC	Motion capture system, calculation of ground truth energy as a function of running speed before and after the turn	• Good results for classifying the turning direction with all models (accuracy > 98.4%) • Support vector regression and neural networks performed best in estimating mechanical work (R^2 = 0.42 – 0.43, MAE = 1.14 – 1.41 J) and running speed

Nr.	Reference	ML approach	Input	Dataset split	Validation	Biomechanical output	Evaluation	Reference data	Key findings
									before/ after the turns (R^2= 0.66 - 0.69, MAE = 0.15-018 m/s)
42	Zangene et al. (2021)	LSTM, a classic multilayer perceptron model for comparison PCA to investigate the effects of different loads on kinematic signals	EMG data matrix from the five electrodes	Training/test: 18/1 participant	Training and testing using k-fold CV, LOSOCV	Knee and ankle angles	RMSE, r	Joint kinematics from IMUs	LSTM accuracy for knee and ankle: • RMSE = 6.774 ± 1.197 and 6.961 ± 1.200, respectively • 3.8% and 4.7% better prediction using cross-correlation method for inputs to the LSTM

NR: not reported in the study.

Discussion

This review examined the use of wearable sensors combined with ML for field-based biomechanical load assessment in sports. Key findings were: (1) Most studies focused on running, with limited research on other sports. (2) IMUs were the most commonly used sensors, typically placed on the thighs, lower legs, and feet. (3) Supervised ML dominated, particularly linear regression and ANNs: unsupervised methods were rarely used. (4) biomechanical load was most frequently investigated using GRF metrics, followed by joint moment metrics and variables characterizing movement execution.

Summary and Validity of Wearable Sensor-ML Approaches

Across the included studies, combinations of wearable sensors and ML showed generally good validity for estimating biomechanical load metrics under controlled conditions, particularly for vertical GRFs and lower-limb joint moments. Validity was commonly quantified by comparing estimates from wearable sensor- and ML to laboratory-based reference data (primarily force plates or force-measuring treadmills, 3D motion capture with inverse dynamics, and musculoskeletal models), within various cross-validation and training approaches. Studies typically used error metrics such as RMSE and normalized RMSE, and agreement measures including correlation coefficients (r, R^2). Many approaches achieved high correlations (often r or $R^2 \geqslant 0.8$-0.9) and relatively low errors (e.g. RMSE of 0.02-0.2 body weights, normalized RMSE of 5-10%) for GRF waveforms and discrete load metrics (e.g. loading rate). For classification and clustering tasks (e.g. high vs. low knee adduction moment, or functional groupings), approaches also typically showed good performance, with accuracies often above 80-90% and area under curve values frequently above 0.8. Validity for more complex quantities (e.g. joint moments, tibial bone forces) and under more variable conditions was more heterogeneous, with accuracy depending on the specific sensor configuration, modelling approach, and whether ML models were participant-specific or participant-independent. Overall, this systematic overview suggests that wearable sensor-ML combinations are a promising tool for estimating biomechanical loads and may provide sufficiently accurate surrogates for laboratory-based methods in some application scenarios, while also highlighting the need for further validation in ecologically valid settings to improve generalizability.

Diversity of Sport Contexts

This review identified running as the most frequently studied sport when applying wearable sensors and ML for field-based biomechanical load assessment. Its prominence is likely due to its broad relevance across various sports and relatively easily accessible biomechanics, which facilitate analysis with field-based wearable sensors. This also minimizes susceptibility to motion capture errors that often increase with more complex movements (Camomilla et al., 2018). However, this narrow focus limits the generalizability of the current work. Although promising results were reported for more complex or sport-specific tasks, such as in soccer (Benjaminse et al., 2024; Di Paolo et al., 2023; Lozano-Berges et al., 2019; Zago et al., 2019) and basketball (Long et al., 2024), these sports remain underrepresented. Upper extremity-dominant sports such as golf, cricket, and hammer throw were addressed in only three studies (Joo et al., 2016; McGrath et al., 2023; Wang et al., 2022), highlighting a gap in the literature. Furthermore, while ten additional sports were included, most were represented by only a single study, limiting the breadth of available evidence. This lack of sport diversity, compounded by small sample sizes, hampers cross-study comparisons. To improve the ecological validity and practical application of wearable sensor and ML-based biomechanical load assessment broader research is needed. For example, by considering a larger number of sports, especially those involving multidirectional, upper body or sport-specific movements. There is also a need for further research in sports such as handball or basketball where high loads are required to optimally control

the training load and improve performance as well as anticipate overloads and reduce their likelihood.

Wearable Sensors and ML Focus and Gaps

IMUs were the most frequently used wearable sensors. Their portability, cost-efficiency, and suitability for field-based applications likely explain their widespread adoption (Ancillao et al., 2018; Camomilla et al., 2018; Picerno, 2017). Sensors were primarily placed on the lower extremities, especially the thighs, lower legs, and feet, reflecting the sports and movements commonly studied. However, sensor placement on the upper limbs was rare, underscoring a gap in investigating sports involving upper extremity-dominant actions such as golf, cricket, or throwing events.

Supervised ML approaches were used in over 90% of studies, predominantly for assessing biomechanical load in terms of GRF metrics. Linear regression and ANNs were the most common techniques, aligning with trends noted in previous literature (Mundt, 2023). Although some studies tested different approaches to select the one with the best results, there is often a lack of comparative studies that systematically test different ML methods or architectures against each other. This usually leaves open the question of whether alternative models or optimized hyperparameter tuning could lead to better prediction results. Unsupervised ML has rarely been used, although under field conditions it offers the advantage of not relying on labeled output data from reference systems such as force plates (Bunker & Thabtah, 2019). As with Lozano-Berges et al. (2019), unsupervised approaches can be used to form patterns, categories and clusters to distinguish between loading or fatigue conditions, for example. Their underuse represents an opportunity for future research to improve ecological validity and reduce reliance on Motion capture systems. Furthermore, studies that systematically compare the predictive power and practicality of supervised and unsupervised learning are still lacking. Such a comparison would be important to better understand where unsupervised approaches offer added value and what methodological trade-offs are involved.

Target Variables and Levels of Biomechanical Load

Biomechanical load was most frequently assessed using GRF metrics. While GRF is valuable due to its relevance across many sports and compatibility with wearable sensor inputs, it represents a global rather than joint or tissue-specific metric (Verheul et al., 2020). However, recent studies have shifted toward predicting internal load metrics such as joint moments, and even tissue stress (Van Hooren et al., 2024). This trend suggests growing interest in structural-level load modeling, a promising direction for future field-based biomechanical research (Stetter & Stein, 2024). Additionally, surface EMG has the potential to assess muscle-specific load, complementing joint kinematic and kinetic data provided by IMUs. By capturing muscle activity directly, EMG can offer insights into muscle strain and fatigue, providing a more detailed understanding of biomechanical loads at the tissue level. This could further refine load assessment and improve injury prevention strategies in sport. Nevertheless, the selection of measurement variables and sensor configurations should always be in line with the respective research question to ensure a practical balance between measurement complexity, and the quality of the load metric. Future research could focus on methods to reliably predict high-quality internal load metrics (e.g. joint contact forces) with a sensor configuration that is as minimal and practicable as possible.

Application-Oriented Patterns in Sports, Sensor Types, ML Approaches, and Target Load Metrics

Taken together, the findings of this study indicate that specific combinations of sports, wearable sensors, ML approaches, and target load metrics cluster around particular biomechanical applications. Field-based estimation of GRFs is predominantly addressed in running, typically using IMUs placed on the pelvis (Bogaert et al., 2024) or lower legs (Derie et al., 2020),

together with supervised ML models such as linear regression or ANNs. When joint moments or tissue-level loads are targeted, studies employ configurations ranging from single IMUs (Long et al., 2024) to multiple IMUs (Dorschky et al., 2020) and apply more complex modelling approaches for both biomechanical load estimation and ML (e.g., Van Hooren et al., 2024), reflecting to some degree the higher dimensionality and nonlinearity of these problems. This pattern suggests that simpler sensor-ML setups may be sufficient for global or impact-related load metrics, whereas joint- or tissue-specific loads may require richer sensor configurations and more advanced models. From a biomechanical perspective, this emphasis on lower-limb loading is reasonable because most sports are performed in bipedal locomotion and the primary external forces act on the lower extremities (Verheul et al., 2020). However, this does not necessarily imply that these approaches are equally applicable to movements involving rapid changes of direction, as seen in team sports such as soccer (Lozano-Berges et al., 2019) and basketball (Long et al., 2024). At the same time, the strong dominance of running, lower-limb sensor placements, supervised learning, and GRF-focused outcomes highlights substantial gaps, particularly for upper-extremity and complex sport-specific tasks, and underscores the need for future work to test alternative wearable sensor-ML combinations in under-represented sports and movement patterns.

Limitations of Reviewed Studies

Several limitations were identified in the studies examined. The lack of diversity in the included sports limits generalizability and reduces comparability between the studies. Another important limitation is the small sample size, which limits the generalization and applicability of the results. In addition, the ML approaches differed greatly in terms of input, for example determined by the number of IMUs, model architecture and biomechanical outputs, making direct comparison difficult. The targeted biomechanical outputs were often sport-specific, further hampering comparability.

Limitations of This Review

This review also has limitations. The search was conducted by a single author, which may introduce selection bias and does not fully meet PRISMA standards. No formal quality assessment was performed due to methodological heterogeneity. The literature search was limited to English-language studies in PubMed and SPORTDiscus, which may have omitted relevant studies, but the references of the included studies were checked to minimize error. Finally, this review is based on a literature search that was last updated in March 2025, and the combination of wearable sensors and ML for biomechanical load estimation is a rapidly evolving field. More recent studies may therefore not be captured, and regular updates of the literature base will be necessary to keep pace with ongoing research.

Conclusion

This study reviewed current practices and trends in the application of wearable sensors and ML for field-based biomechanical load assessment in sports. Since the research predominantly focused on running, there is a clear need to expand investigations to a broader range of sports, particularly those involving complex, multidirectional, or upper body movements. Although GRF remains the most commonly-predicted load metric, current studies are shifting toward more specific metrics, such as joint moments and tissue-level stresses. Future research should aim to refine these models, particularly for predicting structural and tissue-specific loads in field settings. Expanding the diversity of sports studied and improving sensor placement on the upper extremities will be essential to enhance the ecological validity and practical application of wearable sensors in athlete monitoring and injury prevention.

References

Alcantara, R. S., Day, E. M., Hahn, M. E., & Grabowski, A. M. (2021). Sacral acceleration can predict whole-body kinetics and stride kinematics across running speeds. *PeerJ*, *9, e11199*. https://doi.org/10.7717/peerj.11199

Alcantara, R. S., Edwards, W. B., Millet, G. Y., & Grabowski, A. M. (2022). Predicting continuous ground reaction forces from accelerometers during uphill and downhill running: A recurrent neural network solution. *PeerJ*, *10*, 12752. https://doi.org/10.7717/peerj.12752

Ancillao, A., Tedesco, S., Barton, J., & O'Flynn, B. (2018). Indirect measurement of ground reaction forces and moments by means of wearable inertial sensors: A systematic review. *Sensors*, *18*(8), 2564. https://doi.org/10.3390/s18082564

Benjaminse, A., Nijmeijer, E. M., Gokeler, A., & Paolo, S. (2024). Application of machine learning methods to investigate joint load in agility on the football field: Creating the model, Part I. *Sensors*, *24*(11), 3652. https://doi.org/10.3390/s24113652

Billing, D. C., Nagarajah, C. R., Hayes, J. P., & Baker, J. (2006). Predicting ground reaction forces in running using micro-sensors and neural networks. *Sports Engineering*, *9*(1), 15–27. https://doi.org/10.1007/BF02844259

Bogaert, S., Davis, J., & Vanwanseele, B. (2024). Predicting vertical ground reaction force characteristics during running with machine learning. *Frontiers in Bioengineering and Biotechnology*, *12*, 1440033. https://doi.org/10.3389/fbioe.2024.1440033

Bolus, N. B., Jeong, H. K., Blaho, B. M., Safaei, M., Young, A. J., & Inan, O. T. (2021). Fit to burst: Toward noninvasive estimation of achilles tendon load using burst vibrations. *IEEE Transactions on Biomedical Engineering*, *68*(2), 470–481. https://doi.org/10.1109/TBME.2020.3005353

Bunker, R. P., & Thabtah, F. (2019). A machine learning framework for sport result prediction. *Applied Computing and Informatics*, *15*(1), 27–33. https://doi.org/10.1016/j.aci.2017.09.005

Camomilla, V., Bergamini, E., Fantozzi, S., & Vannozzi, G. (2018). Trends supporting the in-field use of wearable inertial sensors for sport performance evaluation: A systematic review. *Sensors*, *18*(3), 873. https://doi.org/10.3390/s18030873

Cerfoglio, S., Galli, M., Tarabini, M., Bertozzi, F., Sforza, C., & Zago, M. (2021). Machine learning-based estimation of ground reaction forces and knee joint kinetics from inertial sensors while performing a vertical drop jump. *Sensors*, *21*(22), 7709. https://doi.org/10.3390/s21227709

Chaaban, C. R., Berry, N. T., Armitano-Lago, C., Kiefer, A. W., Mazzoleni, M. J., & Padua, D. A. (2021). Combining inertial sensors and machine learning to predict vGRF and knee biomechanics during a double limb jump landing task. *Sensors*, *21*(13), 4383. https://doi.org/10.3390/s21134383

Chen, T., Xu, D., Zhou, Z., Zhou, H., Shao, S., & Gu, Y. (2025). Prediction of vertical ground reaction forces under different running speeds: Integration of wearable IMU with CNN-xLSTM. *Sensors*, *25*(4). https://doi.org/10.3390/s25041249

Claudino, J. G., Capanema, D. de O., Souza, T. V., Serrão, J. C., Machado Pereira, A. C., & Nassis, G. P. (2019). Current approaches to the use of artificial intelligence for injury risk assessment and performance prediction in team sports: A systematic review. *Sports Medicine - Open*, *5*(1), 28. https://doi.org/10.1186/s40798-019-0202-3

Cust, E. E., Sweeting, A. J., Ball, K., & Robertson, S. (2019). Machine and deep learning for sport-specific movement recognition: A systematic review of model development and performance. *Journal of Sports Sciences*, *37*(5), 568–600.

Derie, R., Robberechts, P., Berghe, P., Gerlo, J., Clercq, D., Segers, V., & Davis, J. (2020). Tibial acceleration-based prediction of maximal vertical loading rate during overground running: A machine learning approach. *Frontiers in Bioengineering and Biotechnology*, *8*. https://doi.org/10.3389/fbioe.2020.00033

Di Paolo, S., Nijmeijer, E. M., Bragonzoni, L., Gokeler, A., & Benjaminse, A. (2023). Definition of high-risk motion patterns for female ACL injury based on football-specific field data: A wearable sensors plus data mining approach. *Sensors*, *23*(4), 2176. https://doi.org/10.3390/s23042176

Dindorf, C., Bartaguiz, E., Gassmann, F., & Fröhlich, M. (Eds.). (2024). *Artificial intelligence in sports, movement, and health*. Springer.

Donahue, S. R., & Hahn, M. E. (2023a). Estimation of gait events and kinetic waveforms with wearable sensors and machine learning when running in an unconstrained environment. *Scientific Reports*, *13*(1), 2339. https://doi.org/10.1038/s41598-023-29314-4

Donahue, S. R., & Hahn, M. E. (2023b). Estimation of ground reaction force waveforms during fixed pace running outside the laboratory. *Frontiers in Sports and Active Living*, *5*. https://doi.org/10.3389/fspor.2023.974186

Dorschky, E., Nitschke, M., Martindale, C. F., Bogert, A. J., Koelewijn, A. D., & Eskofier, B. M. (2020). CNN-based estimation of sagittal plane walking and running biomechanics from measured and simulated inertial sensor data. *Frontiers in Bioengineering and Biotechnology*, *8*. https://doi.org/10.3389/fbioe.2020.00604

Ferber, R., Osis, S. T., Hicks, J. L., & Delp, S. L. (2016). Gait biomechanics in the era of data science. *Journal of Biomechanics*, *49*(16), 3759–3761. https://doi.org/10.1016/j.jbiomech.2016.10.033

García-de-Villa, S., Casillas-Pérez, D., Jiménez-Martín, A., & García-Domínguez, J. J. (2023). Inertial sensors for human motion analysis: A comprehensive review. *IEEE Transactions on Instrumentation and Measurement*, *72*, 1–39. https://doi.org/10.1109/TIM.2023.3276528

Hajizadeh, M., Clouthier, A. L., Kendall, M., & Graham, R. B. (2023). Predicting vertical and shear ground reaction forces during walking and jogging using wearable plantar pressure insoles. *Gait & Posture*, *104*, 90–96. https://doi.org/10.1016/j.gaitpost.2023.06.006

Halilaj, E., Rajagopal, A., Fiterau, M., Hicks, J. L., Hastie, T. J., & Delp, S. L. (2018). Machine learning in human movement biomechanics: Best practices, common pitfalls, and new opportunities. *Journal of Biomechanics*, *81*, 1–11. https://doi.org/10.1016/j.jbiomech.2018.09.009

Hendry, D., Leadbetter, R., McKee, K., Hopper, L., Wild, C., O'Sullivan, P., Straker, L., & Campbell, A. (2020). An exploration of machine-learning estimation of ground reaction force from wearable sensor data. *Sensors*, *20*(3), 740. https://doi.org/10.3390/s20030740

Hernandez, V., Dadkhah, D., Babakeshizadeh, V., & Kulić, D. (2021). Lower body kinematics estimation from wearable sensors for walking and running: A deep learning approach. *Gait & Posture*, *83*, 185–193. https://doi.org/10.1016/j.gaitpost.2020.10.026

Honert, E. C., Hoitz, F., Blades, S., Nigg, S. R., & Nigg, B. M. (2022). Estimating running ground reaction forces from plantar pressure during graded running. *Sensors*, *22*(9), 3338. https://doi.org/10.3390/s22093338

Joo, S.-B., Oh, S. E., & Mun, J. H. (2016). Improving the ground reaction force prediction accuracy using one-axis plantar pressure: Expansion of input variable for neural network. *Journal of Biomechanics*, *49*(14), 3153–3161. https://doi.org/10.1016/j.jbiomech.2016.07.029

Krumm, D., Kuske, N., Neubert, M., Buder, J., Hamker, F., & Odenwald, S. (2021). Determining push-off forces in speed skating imitation drills. *Sports Engineering*, *24*(1), 25. https://doi.org/10.1007/s12283-021-00362-1

Lang, S., Yang, J., Zhang, Y., Li, P., Gou, X., Chen, Y., Li, C., & Zhang, H. (2025). Application of wearable insole sensors in in-place running: Estimating lower limb load using machine learning. *Biosensors*, *15*(2), 83. https://doi.org/10.3390/bios15020083

Lee, C. J., & Lee, J. K. (2022). Inertial motion capture-based wearable systems for estimation of joint kinetics: A systematic review. *Sensors*, *22*(7), 2507. https://doi.org/10.3390/s22072507

Long, T., Outerleys, J., Yeung, T., Fernandez, J., Bouxsein, M. L., Davis, I. S., Bredella, M. A., & Besier, T. F. (2024). Predicting ankle and knee sagittal kinematics and kinetics using an ankle-mounted inertial sensor. *Computer Methods in Biomechanics and Biomedical Engineering*, *27*(9). https://doi.org/10.1080/10255842.2023.2224912

Lozano-Berges, G., Matute-Llorente, Á., Gómez-Bruton, A., Alfaro-Santafé, V., González-Agüero, A., Vicente-Rodríguez, G., & Casajús, J. A. (2019). Plantar pressures in male adolescent soccer players and its associations with bone geometry and strength. *The Journal of Sports Medicine and Physical Fitness*, *59*(10). https://doi.org/10.23736/S0022-4707.19.09267-3

McGrath, J. W., Neville, J., Stewart, T., Lamb, M., Alway, P., King, M., & Cronin, J. (2023). Can an inertial measurement unit, combined with machine learning, accurately measure ground reaction forces in cricket fast bowling? *Sports Biomechanics*. https://doi.org/10.1080/14763141.2023.2275251

Moore, S. R., Kranzinger, C., Fritz, J., Stöggl, T., Kröll, J., & Schwameder, H. (2020). Foot strike angle prediction and pattern classification using LoadsolTM wearable sensors: A comparison of machine learning techniques. *Sensors*, *20*(23), 6737. https://doi.org/10.3390/s20236737

Mundt, M. (2023). Bridging the lab-to-field gap using machine learning: A narrative review. *Sports Biomechanics*, *1–20*. https://doi.org/10.1080/14763141.2023.2200749

Ngoh, K. J.-H., Gouwanda, D., Gopalai, A. A., & Chong, Y. Z. (2018). Estimation of vertical ground reaction force during running using neural network model and uniaxial accelerometer. *Journal of Biomechanics*, *76*, 269–273. https://doi.org/10.1016/j.jbiomech.2018.06.006

Patoz, A., Lussiana, T., Breine, B., Gindre, C., & Malatesta, D. (2023). Comparison of different machine learning models to enhance sacral acceleration-based estimations of running stride temporal variables and peak vertical ground reaction force. *Sports Biomechanics*. https://doi.org/10.1080/14763141.2022.2159870

Picerno, P. (2017). 25 years of lower limb joint kinematics by using inertial and magnetic sensors: A review of methodological approaches. *Gait & Posture*, *51*, 239–246. https://doi.org/10.1016/j.gaitpost.2016.11.008

Play, M.-C., Giandolini, M., Ravel, A., Millet, G. Y., & Rossi, J. (2024). Effect of midsole hardness on soft tissue vibrations: An ascendant hierarchical clustering on 133 runners. *Scandinavian Journal of Medicine & Science in Sports*, *34*(12). https://doi.org/10.1111/sms.14765

Pogson, M., Verheul, J., Robinson, M. A., Vanrenterghem, J., & Lisboa, P. (2020). A neural network method to predict task- and step-specific ground reaction force magnitudes from trunk accelerations during running activities. *Medical Engineering & Physics*, *78*, 82–89. https://doi.org/10.1016/j.medengphy.2020.02.002

Rattanakoch, J., Samala, M., Limroongreungrat, W., Guerra, G., Tharawadeepimuk, K., Nanbancha, A., Niamsang, W., Kerdsomnuek, P., & Suwanmana, S. (2023). Validity and reliability of inertial measurement unit (IMU)-derived 3D joint kinematics in persons wearing transtibial prosthesis. *Sensors*, *23*(3). https://doi.org/10.3390/s23031738

Song, B., Paolieri, M., Stewart, H. E., Golubchik, L., McNitt-Gray, J. L., Misra, V., & Shah, D. (2025). Estimating ground reaction forces from inertial sensors. *IEEE Transactions on Biomedical Engineering*, *72*(2), 595–608. https://doi.org/10.1109/TBME.2024.3465373

Stetter, B. J., Krafft, F. C., Ringhof, S., Stein, T., & Sell, S. (2020). A machine learning and wearable sensor based approach to estimate external knee flexion and adduction moments during various locomotion tasks. *Frontiers in Bioengineering and Biotechnology*, *8*. https://doi.org/10.3389/fbioe.2020.00009

Stetter, B. J., Ringhof, S., Krafft, F. C., Sell, S., & Stein, T. (2019). Estimation of knee joint forces in sport movements using wearable sensors and machine learning. *Sensors*, *19*(17), 3690. https://doi.org/10.3390/s19173690

Stetter, B. J., & Stein, T. (2024). Machine learning in biomechanics: Enhancing human movement analysis. In C. Dindorf, E. Bartaguiz, F. Gassmann, & M. Fröhlich (Eds.), *Artificial intelligence in sports, movement, and health* (pp. 139–160). Springer Nature Switzerland. https://doi.org/10.1007/978-3-031-67256-9_9

Sun, T., Li, D., Fan, B., Tan, T., & Shull, P. B. (2023). Real-time ground reaction force and knee extension moment estimation during drop landings via modular LSTM modeling and wearable IMUs. *IEEE Journal of Biomedical and Health Informatics*, *27*(7), 3222–3233. https://doi.org/10.1109/JBHI.2023.3268239

Tan, T., Strout, Z. A., Cheung, R. T. H., & Shull, P. B. (2022). Strike index estimation using a convolutional neural network with a single, shoe-mounted inertial sensor. *Journal of Biomechanics*, *139*, 111145. https://doi.org/10.1016/j.jbiomech.2022.111145

Tan, T., Strout, Z. A., & Shull, P. B. (2021). Accurate impact loading rate estimation during running via a subject-independent convolutional neural network model and optimal IMU placement. *IEEE Journal of Biomedical and Health Informatics*, *25*(4). https://doi.org/10.1109/JBHI.2020.3014963

Uddin, M. Z., Seeberg, T. M., Kocbach, J., Liverud, A. E., Gonzalez, V., Sandbakk, Ø., & Meyer, F. (2021). Estimation of mechanical power output employing deep learning on inertial measurement data in roller ski skating. *Sensors*, *21*(19), 6500. https://doi.org/10.3390/s21196500

Van Hooren, B., Rengs, L., & Meijer, K. (2024). Predicting musculoskeletal loading at common running injury locations using machine learning and instrumented insoles. *Medicine and Science in Sports and Exercise*, *56*(10). https://doi.org/10.1249/MSS.0000000000003493

Vanrenterghem, J., Nedergaard, N. J., Robinson, M. A., & Drust, B. (2017). Training load monitoring in team sports: A novel framework separating physiological and biomechanical load-adaptation pathways. *Sports Medicine*, *47*(11), 2135–2142. https://doi.org/10.1007/s40279-017-0714-2

Verheul, J., Nedergaard, N. J., Vanrenterghem, J., & Robinson, M. A. (2020). Measuring biomechanical loads in team sports – from lab to field. *Science and Medicine in Football*, *4*(3), 246–252. https://doi.org/10.1080/24733938.2019.1709654

Wang, Y., Shan, G., Li, H., & Wang, L. (2022). A wearable-sensor system with AI technology for real-time biomechanical feedback training in hammer throw. *Sensors*, *23*(1), 425.

Wouda, F. J., Giuberti, M., Bellusci, G., Maartens, E., Reenalda, J., Beijnum, B.-J. F., & Veltink, P. H. (2018). Estimation of vertical ground reaction forces and sagittal knee kinematics during running using three inertial sensors. *Frontiers in Physiology*, *9*. https://doi.org/10.3389/fphys.2018.00218

Xiang, L., Gu, Y., Wang, A., Shim, V., Gao, Z., & Fernandez, J. (2023). Foot pronation prediction with inertial sensors during running: A preliminary application of data-driven approaches. *Journal of Human Kinetics*, *88*, 29–40. https://doi.org/10.5114/jhk/163059

Xiang, L., Wang, A., Gu, Y., Zhao, L., Shim, V., & Fernandez, J. (2022). Recent machine learning progress in lower limb running biomechanics with wearable technology: A systematic review. *Frontiers in Neurorobotics*, *16*. https://doi.org/10.3389/fnbot.2022.913052

Yılmazgün, B., Weber, J., Stein, T., Sell, S., & Stetter, B. J. (2025). Predicting 3D ground reaction forces across various movement tasks: A convolutional neural network study comparing different inertial measurement unit configurations. *Journal of Biomechanics*, *112888*. https://doi.org/10.1016/j.jbiomech.2025.112888

Zago, M., Sforza, C., Dolci, C., Tarabini, M., & Galli, M. (2019). Use of machine learning and wearable sensors to predict energetics and kinematics of cutting maneuvers. *Sensors*, *19*(14), 3094. https://doi.org/10.3390/s19143094

Zangene, A. R., Abbasi, A., & Nazarpour, K. (2021). Estimation of lower limb kinematics during squat task in different loading using sEMG activity and deep recurrent neural networks. *Sensors*, *21*(23), 7773. https://doi.org/10.3390/s21237773

Zhou, D., Keogh, J. W., Ma, Y., Tong, R. K., Khan, A. R., & Jennings, N. R. (2025). Artificial intelligence in sport: A narrative review of applications, challenges and future trends. *Journal of Sports Sciences*, 1–16.

Acknowledgements

Funding

The authors have no funding or support to report.

Competing interests

The authors have declared that no competing interests exist.

Data availability statement

All relevant data are within the paper.